TSI Press Series

FIRST INDUSTRY/ACADEMY SYMPOSIUM ON RESEARCH FOR FUTURE SUPERSONIC AND HYPERSONIC VEHICLES

Applications, Design, Development, and Research

Held December 4-6, 1994 in Greensboro, North Carolina, U.S.A.

Volume 1

Editors:

Abdollah Homaifar
Department of Electrical Engineering
North Carolina A&T State University

John C. Kelly, Jr.
Department of Electrical Engineering
North Carolina A&T State Unversity

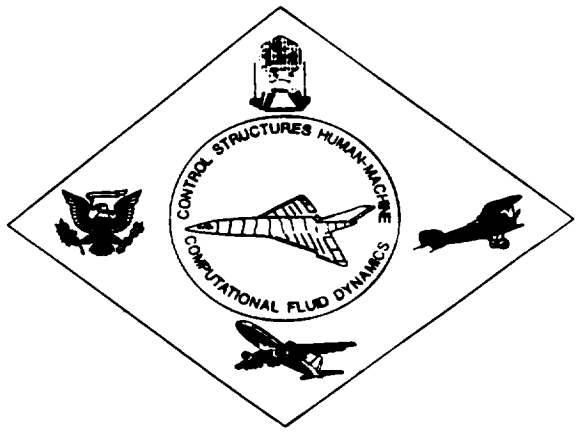

TSI Press Albuquerque, New Mexico USA 1994

DYNAMIC BEHAVIOR OF A MAGNETIC BEARING SUPPORTED JET ENGINE ROTOR WITH AUXILIARY BEARINGS

G.T. Flowers
H. Xie
S.C. Sinha

Department of Mechanical Engineering
Auburn University
Auburn, Alabama

ABSTRACT

This paper presents a study of the dynamic behavior of a rotor system supported by auxiliary bearings. The steady–state behavior of a simulation model based upon a production jet engine is explored over a wide range of operating conditions for varying rotor imbalance, support stiffness and damping. Interesting dynamical phenomena, such as chaos, subharmonic responses, and double–valued responses, are presented and discussed.

KEYWORDS: magnetic bearings, auxiliary bearings, nonlinear rotordynamics.

NOMENCLATURE

C_B = auxiliary bearing support damping, lb.s/in.
F_n = normal force, lb
$\mathbf{F}_X$ = external force vector acting on the rotor in X direction
$\mathbf{F}_Y$ = external force vector acting on the rotor in Y direction
$\mathbf{I}_a$ = rotor inertia matrix
K_B = auxiliary bearing support stiffness, lb/in.
K_C = contact stiffness, lb/in.
M_B = auxiliary bearing mass, lb.s^2/in.
M_k = mass of kth rotor element, lb.s^2/in.
N = total number of modes considered
N_{B1} = node number at auxiliary bearing #1
N_{B2} = node number at auxiliary bearing #2
$\mathbf{Q}_X$ = rotor modal coordinate vector in X direction
$\mathbf{Q}_Y$ = rotor modal coordinate vector in Y direction
R_B = radius of auxiliary bearing bore, in.
R_R = radius of rotor journal, in.
$\mathbf{X}_R$ = rotor physical coordinate vector in X direction
$\mathbf{Y}_R$ = rotor physical coordinate vector in Y direction
e = rotor imbalance eccentricity, in.
g = gravitational acceleration, in./s^2
t = time, s
Δ = deformation at the contact point, in.
$\mathbf{\Gamma} = \mathbf{\Psi}^T \mathbf{I}_a \mathbf{\Psi}$
$\mathbf{\Psi}$ = rotor free-free modal rotation matrix
Ω = rotor operating speed, rad/s
$\mathbf{\Phi}$ = rotor free-free modal displacement matrix
$\delta = R_B - R_R$, auxiliary bearing clearance, in.

ζ = modal damping coefficient

INTRODUCTION

Active magnetic bearings are one of the most innovative recent developments in the turbomachinery field. This technology provides the potential for significant improvements over other types of rotor support, including elimination of wear and bearing friction–related energy losses as well as a means of actively suppressing rotor vibration. A critical component of any magnetic bearing design is the auxiliary bearing, which protects the soft iron core of the magnetic bearing and provides rotor support in case of overload or failure of the primary (magnetic) bearing. Magnetic bearing systems appear to provide particularly great promise for use in aeronautical applications. In this regard, current effort is directed toward developing jet engines with rotors supported by magnetic bearings. For such applications, safety is an important concern. Toward this end, it is desirable to design the system to operate with auxiliary bearing support for an extended period of time.

A number of different bearing types have been suggested as auxiliary bearings. These include bushings, rolling element bearings, and various types of journal bearings. The most commonly considered are rolling element bearings. The major disadvantage associated with using rolling element bearings (or bushings) is the requirement of a clearance between the rotor and the inner race of the bearing, without which many of the advantages associated with using magnetic bearings would be reduced or eliminated. This clearance introduces a nonlinear dynamical feature which may significantly impact the behavior of the rotor.

There are quite a number of studies in the literature concerned with nonlinear rotordynamics. Yamamoto (1954) conducted a systematic study of rotor responses involving bearing clearance effects. Black (1968) studied the rotor/stator interaction with a clearance. Ehrich (1966, 1988 and 1991), Bently (1974), Muszynska (1984) and Childs (1979 and 1982) observed and studied subharmonic responses associated with clearance effects. While this work has served to greatly enhance the understanding of such systems, more detailed study is needed. Much of this earlier work was conducted from the perspective that the clearance is a result of manufacturing error or misfitting and is best eliminated. However, in a rotor system fitted with magnetic bearings and auxiliary bearings, the clearance becomes a design parameter rather than an irregularity. From this point of view, it is important to develop a better understanding of the expected dynamic responses. Such knowledge will provide guidelines for the selection of auxiliary bearing parameters.

There has been relatively little work available in the open literature that is specifically concerned with auxiliary bearings. Two papers that are directly related to research on auxiliary bearings are Gelin et al., (1990) and Ishii and Kirk (1991). Both of these papers are mainly concerned with transient responses. The current work is specifically concerned with developing a better understanding of the expected steady–state dynamical behavior for an auxiliary bearing supported rotor. Simulation results for a rotor based upon a production jet engine are presented and discussed.

The model used in the current study has two principal components - the rotor and the auxiliary bearings. The rotor is modelled using the free–free bending mode shapes and natural frequencies obtained through finite element analysis. The finite element code uses 34 stations and the first four modes (two rigid body and two flexible modes) are included in the simulation model. Figure 1 shows a schematic diagram of the finite element model. The rotor equations of motion can be expressed in terms of modal coordinates as:

$$\ddot{\mathbf{Q}}_X + 2\zeta\omega_n\dot{\mathbf{Q}}_X + \Omega\mathbf{\Gamma}\dot{\mathbf{Q}}_Y + \omega_n^2\mathbf{Q}_X + 2\Omega\zeta\omega_n\mathbf{Q}_Y = \mathbf{\Phi}^T\mathbf{F}_X, \tag{1.a}$$

$$\ddot{\mathbf{Q}}_Y + 2\zeta\omega_n\dot{\mathbf{Q}}_Y - \Omega\mathbf{\Gamma}\dot{\mathbf{Q}}_X + \omega_n^2\mathbf{Q}_Y - 2\Omega\zeta\omega_n\mathbf{Q}_X = \mathbf{\Phi}^T\mathbf{F}_Y, \tag{1.b}$$

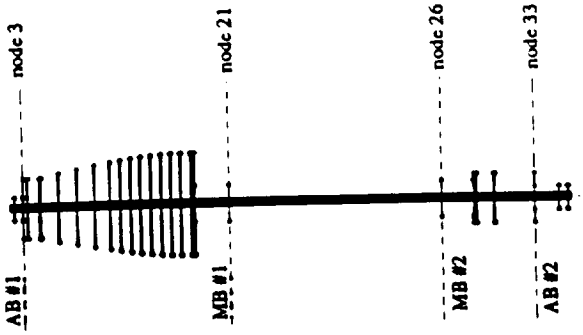

FIGURE 1 DIAGRAM OF THE FINITE ELEMENT MODEL

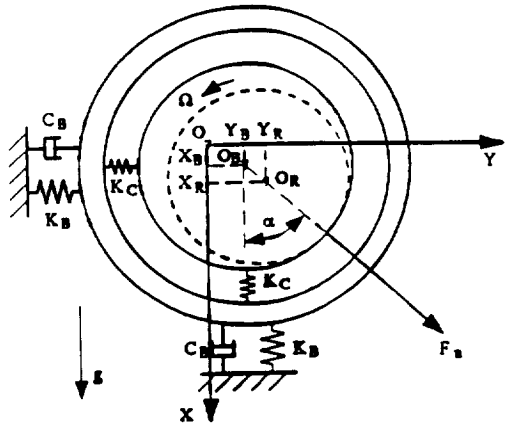

FIGURE 2 AUXILIARY BEARING MODEL

where

$$\mathbf{F}_X = \{F_{X1}, F_{X2}, \ldots, F_{Xm}\}^{-T},$$
$$\mathbf{F}_Y = \{F_{Y1}, F_{Y2}, \ldots, F_{Ym}\}^{-T},$$
$$\mathbf{Q}_X = \Phi^{-1}\mathbf{X}_R,$$
$$\mathbf{Q}_Y = \Phi^{-1}\mathbf{Y}_R,$$
$$\omega_n = \begin{pmatrix} \omega_{n_1} & 0 & \ldots & 0 \\ 0 & \omega_{n_2} & \ldots & 0 \\ \ldots & \ldots & \ldots & \ldots \\ 0 & 0 & \ldots & \omega_{n_N} \end{pmatrix}$$

with

$$\mathbf{X}_R = \{X_{R1}, X_{R2}, \ldots, X_{Rm}\}^{-T},$$
$$\mathbf{Y}_R = \{Y_{R1}, Y_{R2}, \ldots, Y_{Rm}\}^{-T}.$$

(m = total number of nodes)

The physical displacements of the rotor at the two auxiliary bearing locations can be obtained using the following coordinate transformation:

$$X_{Rk} = \sum_{i=1}^{N} \Phi_{ki} Q_{Xi}, \qquad (k = N_{B1}, N_{B2})$$
$$Y_{Rk} = \sum_{i=1}^{N} \Phi_{ki} Q_{Yi},$$

The model for the auxiliary bearings is shown in Figure 2. The governing equations of motion are:

$$M_{Bk}\ddot{X}_{Bk} + C_{Bk}\dot{X}_{Bk} + K_{Bk}X_{Bk} = F_{nk}\cos\alpha_k + M_{Bk}g, \qquad (2.a)$$
$$M_{Bk}\ddot{Y}_{Bk} + C_{Bk}\dot{Y}_{Bk} + K_{Bk}Y_{Bk} = F_{nk}\sin\alpha_k, \qquad (2.b)$$

where

$$\alpha_k = tan^{-1} \frac{Y_{Rk} - Y_{Bk}}{X_{Rk} - X_{Bk}}.$$

$$(k = N_{B1}, N_{B2})$$

$$F_{Xk} = - F_{nk} \cos \alpha_k + M_k \, g + M_k \, e \, \Omega^2 \cos(\Omega t),$$
$$F_{Yk} = - F_{nk} \sin \alpha_k + M_k \, e \, \Omega^2 \sin(\Omega t).$$

The rotor/bearing interaction is represented with the normal force F_{nk}

$$F_{nk} = \begin{cases} K_C \delta_k, & \Delta_k > 0, \\ 0, & \Delta_k \leq 0, \end{cases} \tag{3}$$

where

$$\Delta_k = (X_{Rk} - X_{Bk}) \cos \alpha_k + (Y_{Rk} - Y_{Bk}) \sin \alpha_k - \delta_k.$$

DISCUSSION OF RESULTS

The model described in the previous section was used to study the steady–state dynamic behavior of such a system using direct numerical integration of the equations and a harmonic balance code. Studies were performed for varied values of imbalance, support stiffness, and support damping, respectively. For the purposes of the current work, the two auxiliary bearings are located at nodes 3 and 33, respectively. It is assumed that they are identical in terms of stiffness, damping and friction characteristics. The nominal system parameters used for the simulation study are M_{B1}=0.0023, M_{B2}=0.0024, K_C=2.855e+6, and ζ=0.03. All the results that are presented correspond to node 3, the location of bearing 1.

The dynamical behavior of a rotor supported by bearings with clearance coupled with the nonsymmetry resulting from gravitational effects can be quite complex. The harmonic balance method is first used to investigate the synchronous behavior for small imbalance values. (Please note that the complex frequency contents associated with medium and large imbalance values makes it a formidable task to apply the harmonic balance method for other cases.) Figure 3 is a typical plot of the steady state response amplitudes as functions of the rotor speed with and without bearing clearance. The nonsymmetric effects resulting from gravity loading is similar to what occurs for a rotor supported by nonsymmetric bearing stiffnesses with regard to influence on critical speeds. The first critical speed splits into two distinct values. For the X direction, the gravity force tends to keep the rotor in contact with the bearing at low operating speed. The apparent stiffness in this direction is approximately the same as K_B and the resulting critical speed about the same as the critical speed for the linear case (δ=0). For the Y direction, the clearance results in a lower apparent stiffness and a lower critical speed. Several higher order pseudo-critical speeds are also created in the operating speed range (about 1500 rad./sec). It should be noted that the response in the X direction also departs from the linear case at high operating speed. This is because the imbalance force becomes dominant at high rotor speed which in turn makes the gravity force less significant and the clearance effect more important.

Figure 4(a) shows some typical results for varying imbalance. Some of the more dynamically interesting results occur for cases of relatively large imbalance. It is observed that imbalance may influence the frequency content of the rotor responses quite dramatically at certain operating speeds. There exists as many as eight ranges of imbalance values that result in eight different types of rotor responses. In fact, subharmonic responses from $\Omega/2$ through $\Omega/10$ are observed. Those subharmonics are not directly related to the system's natural frequencies as were the cases with other researchers' findings (such as Ehrich, 1988). Moreover, several types of subharmonic responses may occur for identical parametric configurations, but different imbalance values.

Figures 4(b) and 4(c) show typical results using K_B or C_B as the variable parameter. Clear routes to chaos are observed. As K_B increases beyond certain value, a period-doubling bifurcation always

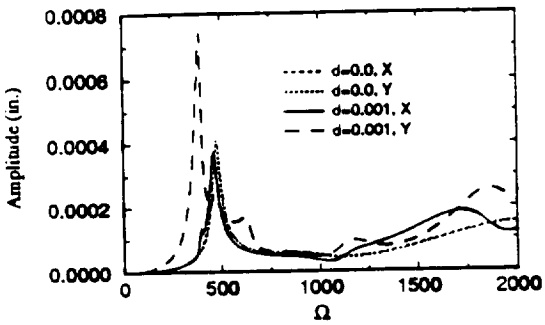

FIGURE 3 INFLUENCE OF CLEARANCE ON CRITICAL SPEEDS
(e=0.0001, C_B=150.0, K_B=0.313x10^6)

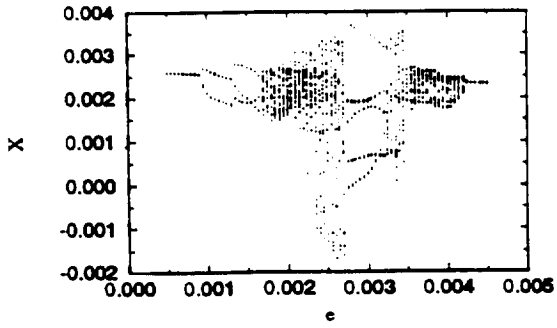

FIGURE 4(a) BIFURCATION DIAGRAM WITH IMBALANCE AS THE VARIABLE PARAMETER
(Ω=1000, δ=0.002, C_B=150, K_B=0.313x10^6)

takes place. As C_B decreases below certain value, the responses always become chaotic. However, the bifurcation type is not well defined as for varied K_B. It should be pointed out that even though a lower K_B may leads to a better system response, it may also fail to protect the magnetic bearings due to the fact that it could result in a larger rotor orbit-center offset. In addition, higher bearing damping does not necessarily result in synchronous responses. It is observed that, with small imbalance ($e \leq 0.0005$), the responses are always synchronous for all speeds in the speed range considered ($\leq$ 1800) if C_B is large enough (C_B=250.0) and the clearance is small enough ($\delta \leq 0.001$). As with the other cases, higher bearing damping or lower bearing stiffness or lower imbalance tends to increase the probability of synchronous responses.

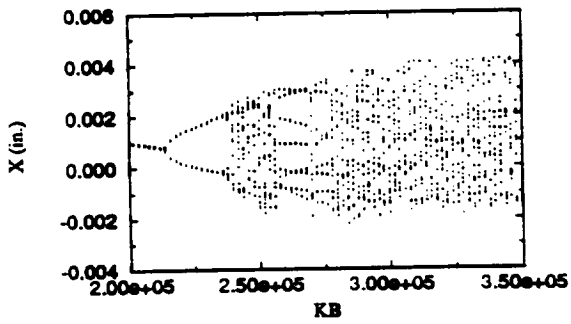

FIGURE 4(b) BIFURCATION DIAGRAM WITH BEARING STIFFNESS AS THE VARIABLE PARAMETER
(Ω=1500, δ=0.002, C_B=150, e=0.0008)

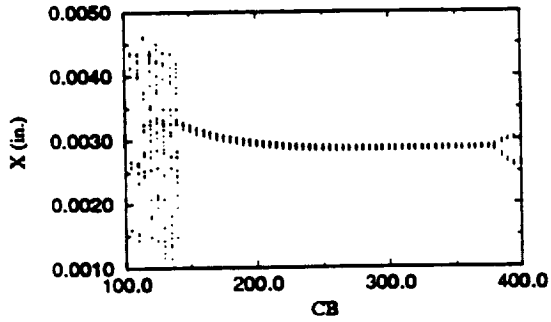

FIGURE 4(c) BIFURCATION DIAGRAM WITH BEARING DAMPING AS THE VARIABLE PARAMETER
(Ω=1500, δ=0.002, e=0.0015, K_B=0.313x10^6)

CONCLUSIONS

As a summary of the results discussed above, the following conclusions can be drawn:

1. Imbalance may serve to dramatically alter the frequency contents of the rotor responses at certain operating speeds. This is particularly evident for cases of large clearance, high bearing stiffness and low bearing damping.
2. For sufficiently high imbalance:
   i. There is a threshold level of damping below which complex dynamical behavior can be expected.
   ii. There is a threshold level of stiffness above which complex dynamical behavior can be expected.
3. Clear routes to chaos are observed. As bearing stiffness increases beyond a certain value, a period-doubling bifurcation takes place which leads to chaos. As bearing damping decreases below a certain value, chaos also tends to occur but the bifurcation type is not so clearly defined.

ACKNOWLEDGEMENT

The authors would like to express their gratitude to S. A. Klusman of the Allison Engine Company for many helpful discussions and practical advice.
This work was supported by NASA under Grant No. NAG3-1507. The Government has certain rights in this material.

REFERENCES

Bently, D. E., 1974, "Forced Subrotative Speed Dynamic Action of Rotating Machinery," ASME Paper No. 74-PET-16.
Black, H. F., 1968, "Interaction of a Whirling Rotor With a Vibrating Stator Across a Clearance Annulus," *Journal of Engineering Science*, Vol. 10, No. 1, pp. 1-12.
Childs, D. W., 1979, "Rub-Induced Parametric Excitation in Rotors," ASME *Journal of Mechanical Design*, Vol. 101, pp. 640-644.
Childs, D. W., 1982, "Fractional-Frequency Rotor Motion Due to Nonsymmetric Clearance Effects," ASME *Journal of Engineering for Power*, Vol. 104, pp. 533-541.
Ehrich, F. F., 1966, "Subharmonic Vibration of Rotors in Bearing Clearance," ASME Paper 66-MD-1.
Ehrich, F. F., 1988, "High Order Subharmonic Response of High Speed Rotors in Bearing Clearance," ASME *Journal of Vibration, Acoustics, Stress, and Reliability in Design*, Vol. 110, pp. 9-16.
Ehrich, F. F., 1991, "Some Observations of Chaotic Vibration Phenomena in High-Speed Rotordynamics," ASME *Journal of Vibration, Acoustics, Stress, and Reliability in Design*, Vol. 113, pp. 50-57.
Gelin, A., Pugnet, J. M., and Hagopian, J. D., 1990, "Dynamic Behavior of Flexible Rotors with Active Magnetic Bearings on Safety Auxiliary Bearings," *Proceedings of 3rd International Conference on Rotordynamics*, Lyon, France, pp. 503-508.
Ishii, T., and Kirk, R. G., 1991, "Transient Response Technique Applied to Active Magnetic Bearing Machinery During Rotor Drop," *DE- Vol. 35, Rotating Machinery and Vehicle Dynamics, ASME*, pp.191-199.
Muszynska, A., 1984, "Partial Lateral Rotor to Stator Rubs," IMechE Paper No. C281/84.
Yamamoto, T. T., 1954, "On Critical Speeds of a Shaft," *Memoirs of the Faculty of Engineering*, Nagoya University (Japan), Vol. 6, No. 2.